Title

Pseudo-single-bunch mode for a 100 MHz storage ring serving soft X-ray timing experiments

Authors

Olsson, T
Leemann, SC
Georgiev, G
et al.

Publication Date

2018-06-01

DOI

10.1016/j.nima.2018.03.067

Peer reviewed

Nuclear Inst. and Methods in Physics Research, A 894 (2018) 145–156

Contents lists available at ScienceDirect

Nuclear Inst. and Methods in Physics Research, A

journal homepage: www.elsevier.com/locate/nima

Pseudo-single-bunch mode for a 100 MHz storage ring serving soft X-ray timing experiments

T. Olsson *, S.C. Leemann [1], G. Georgiev, G. Paraskaki

MAX IV Laboratory, Lund University, SE-22100 Lund, Sweden

ARTICLE INFO

Keywords:
Synchrotron light source
Storage ring
Pseudo single bunch
Timing experiments

ABSTRACT

At many storage rings for synchrotron light production there is demand for serving both high-flux and timing users simultaneously. Today this is most commonly achieved by operating inhomogeneous fill patterns, but this is not preferable for rings that employ passive harmonic cavities to damp instabilities and increase Touschek lifetime. For these rings, inhomogeneous fill patterns could severely reduce the effect of the harmonic cavities. It is therefore of interest to develop methods to serve high-flux and timing users simultaneously without requiring gaps in the fill pattern. One such method is pseudo-single-bunch (PSB), where one bunch in the bunch train is kicked onto another orbit by a fast stripline kicker. The light emitted from the kicked bunch can then be separated by an aperture in the beamline. Due to recent developments in fast kicker design, PSB operation in multibunch mode is within reach for rings that operate with a 100 MHz RF system, such as the MAX IV and Solaris storage rings. This paper describes machine requirements and resulting performance for such a mode at the MAX IV 1.5 GeV storage ring. A solution for serving all beamlines is discussed as well as the consequences of beamline design and operation in the soft X-ray energy range.

1. Introduction

At synchrotron light storage rings there is demand for serving both high-flux and timing users.[2] Maximum average flux is achieved when the storage ring is operated in multibunch mode, but timing users usually require single-bunch repetition rates or lower. To be able to serve both user groups simultaneously many storage rings currently operate with inhomogeneous fill patterns, e.g. fill patterns with a camshaft bunch placed in a gap of sufficient length for operation with beamline choppers. However, for rings that employ passive harmonic cavities (HCs) to damp instabilities and increase Touschek lifetime by lengthening the bunches, operation of inhomogeneous fill patterns is not favorable. Studies performed at several storage rings operating with or planning for passive HCs, e.g. [1–5], show that inhomogeneous fill patterns give rise to transient effects that decrease the average bunch lengthening. It is therefore of interest to develop methods that can deliver suitable repetition rates for timing users while operating the ring in multibunch mode. A few methods that have this potential have been demonstrated or are under development, pseudo-single-bunch (PSB) [6–9], pulse picking by resonant excitation (PPRE) [10] and transverse resonance island buckets (TRIBs) [11,12].

The MAX IV 1.5 GeV storage ring is designed to operate with a 100 MHz RF system and a 500 mA [13] homogeneous multibunch fill pattern [14], but discussions on timing modes have been initiated by the user community. Several research areas have been identified that require kHz–MHz repetition rates which currently cannot be provided at the MAX IV facility [15]. These discussions have led to the submission of a science case for a single-bunch mode at the 1.5 GeV ring [16], but such a mode can only serve timing users a few weeks per year. Therefore other solutions are of interest to increase the beamtime available for timing experiments. The ring employs passive harmonic cavities (HCs) [13,17] and bunch elongation is an essential part of the design. In addition, conventional beamline choppers require a gap of a few hundred ns [18], and since the revolution period of the ring is only 320 ns [14] a gap of sufficient length would result in a substantial decrease in flux for high-flux users. It is therefore preferable to operate the ring with the planned homogeneous multibunch fill pattern to maximize flux to the high-flux

* Corresponding author.
E-mail address: teresia.olsson@maxiv.lu.se (T. Olsson).
[1] New address: Lawrence Berkeley National Laboratory, Berkeley, CA 94720, USA.
[2] Timing users here refers to all users with specific demands on repetition rate and/or pulse length of the light.

https://doi.org/10.1016/j.nima.2018.03.067
Received 16 November 2017; Received in revised form 25 March 2018; Accepted 25 March 2018
Available online 29 March 2018
0168-9002/

Table 1
Parameters of the MAX IV 1.5 GeV ring [14,23].

Energy	1.5 GeV
Main RF frequency	99.931 MHz
Harmonic number	32
Design current	500 mA
Circumference	96 m
Number of achromats	12
Length of straight sections	3.5 m
Betatron tunes (hor./vert.)	11.22/3.15
Beta functions in straights (hor./vert.)	5.692/2.837
Equilibrium emittance (bare lattice)	5.980 nm rad

Table 2
Time structure of the MAX IV 1.5 GeV ring.

Single-bunch repetition rate	3.125 MHz
Bunch spacing in multibunch mode	10 ns
Bunch length (RMS)	49–213 ps[a]

[a] Dependent on stored current, HC tuning, and main RF cavity setting.

users and avoid degrading the performance of the HCs.

The PSB method has been developed and operated for users at ALS in a hybrid fill pattern with a camshaft bunch in a 100 ns gap [6–8]. In this method, one bunch in the bunch train is kicked onto another orbit by a fast stripline kicker. The light from the kicked bunch can then be separated from the light produced by the multibunch train by an aperture in the beamline, resulting in single-bunch light without disturbing high-flux users at other beamlines. The PSB method is of special interest for MAX IV due to the 100 MHz RF system, which provides 10 ns interval between bunches. Ongoing development in fast kicker design has shown pulse lengths which puts PSB operation in a 100 MHz multibunch mode within reach [19,20]. A kicker pulse shorter than 20 ns enables operating PSB in multibunch mode, and serving high-flux and timing users simultaneously without compromising the performance of the HCs, and thus the lifetime and stability of the beam. This is also of wider interest for other storage rings operating with a 100 MHz RF system, such as Solaris [21] or the ultralow emittance MAX IV 3 GeV storage ring and future multibend achromat rings where the performance of passive harmonic cavities is essential for preserving the ultralow emittance [22].

2. Prerequisites for a PSB mode at the MAX IV 1.5 GeV storage ring

The MAX IV 1.5 GeV storage ring is designed to serve UV and soft X-ray users. It has a 96 m double-bend achromat lattice resulting in an emittance of 6 nm rad [17,23]. An overview over the parameters of the ring can be found in Table 1. For timing experiments, three temporal properties are of interest: the repetition rate, the bunch spacing and the bunch length. These properties are listed in Table 2. The ring has so far five funded beamlines, of which FlexPES and FinEstBeAMS beamlines have expressed strong interest for a future timing mode, such as PSB. Furthermore, the ring has five straight sections available for new beamlines. The ring is not planned to include bending magnet beamlines, and thus all beamlines will utilize insertion devices for light production. The photon energy ranges of the five planned beamlines span 4–1500 eV [24–28]. The present energy range of interest of the MAX IV timing user community spans 4–700 eV, but it is possible that higher energies will also be of interest in the future. The required repetition rates at the sample span from tens of kHz to the single-bunch repetition rate of 3.125 MHz [16].

The PSB mode described in this paper utilizes one kicker and, unlike the implementation at ALS, focuses on the optimization of this mode to serve as many beamlines and users as possible. The reasons for relying on a single kicker is the technical challenge to synchronize several kickers and the available space in the ring. In addition, a kick-and-cancel (KAC) design, where the PSB is kicked onto another orbit and then kicked back after a few turns, is pursued. This ensures a well-defined orbit at all times and by adjusting the period between the KAC cycles, the repetition rate of the light seen by the beamlines can be selected [6]. Lower repetition rates than provided by the single-bunch repetition rate can also be supplied by a chopper in the beamline [18] and therefore this paper will also discuss the possible performance gains when operating PSB in combination with choppers. Finally, to conserve the polarization properties of the radiation emitted from the PSB and to enable the beamlines to quickly switch between multibunch and PSB operation without realignment, local orbit bumps which place the PSB on-axis through the insertion devices will be required.

3. Connection between photon beam separation and the electron beam orbit

For user operation of a PSB mode it is essential to achieve sufficient separation between the light from the PSB and the light from the rest of the multibunch train. The photon beam separation can be defined as the distance between the center of the PSB photon beam and the center of the multibunch photon beam. The separation of unfocused photon beams at a distance d from the beamline source point is given by

$$S = u + du', \tag{1}$$

where u and u' are the position and angle of the PSB electron beam centroid at the source point. The separation can be expressed in sigmas of the convoluted photon beam size as $S = N\sigma_d$, where

$$N = \frac{u}{\sigma_d} + d\frac{u'}{\sigma_d} \tag{2}$$

and σ_d is the RMS photon beam size at the distance d from the source point. While the separation at the beamline source point is purely given by the position of the PSB electron orbit, as the distance from the source increases, the angle of the electron orbit becomes the dominating factor for the resulting separation. Therefore, for beamlines in which the source is imaged into an intermediate focus before the monochromator where the separation can be performed with focused photon beams, it is the PSB electron beam position that is of relevance. On the other hand, for beamlines without intermediate focus, where the separation has to be performed with defocused photon beams, both the PSB electron beam position and angle have to be taken into account. Hereafter, these two different principles for separating the light are denoted focused and unfocused separation in reference to the state of the photon beams at the separation point.

For a beamline with an intermediate focus utilizing focused separation of the light, the separation is given by

$$S = N_f\sigma_0, \tag{3}$$

where

$$N_f = \frac{u}{\sigma_0} \tag{4}$$

and σ_0 is the RMS photon beam size at the source. For a beamline without intermediate focus utilizing unfocused separation, the evolution of the beam size along the beamline can be described by Gaussian beam formalism resulting in

$$\sigma_d = d\sigma_0', \tag{5}$$

where σ_0' is the RMS photon beam divergence at the source. The separation at a distance d from the source point is in this case given by

$$S = N_{uf}\sigma_d \tag{6}$$

where

$$N_{uf} = \frac{u}{d\sigma_0'} + \frac{u'}{\sigma_0'}. \tag{7}$$

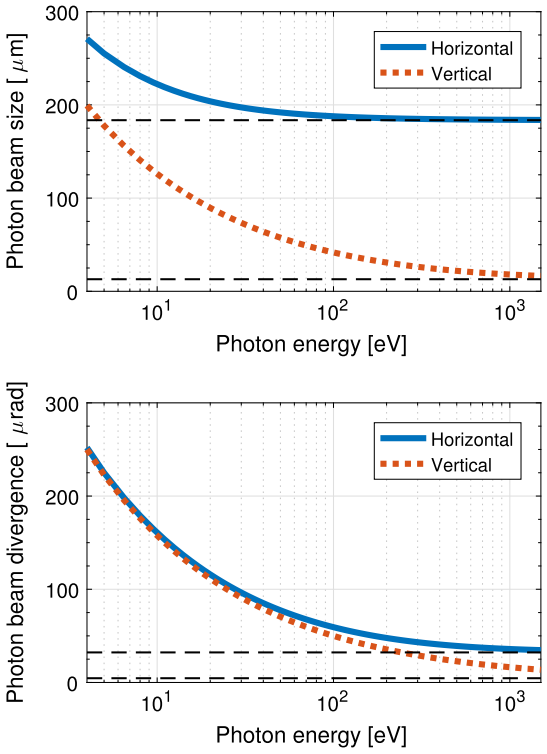

Fig. 1. Approximated convoluted photon beam size and divergence for a 2.5 m undulator as function of photon energy between 4–1500 eV. The dashed lines mark the corresponding electron beam size and divergence.

Comparing Eqs. (4) and (7), it can be noted that the required electron beam orbit is determined by either the photon beam size or divergence at the source depending on the separation method.

Fig. 1 displays the RMS photon beam size and divergence for a 2.5 m undulator as a function of photon energy.[3] It is apparent that for the photon energy range of interest for the MAX IV timing users, the contribution from diffraction to the photon beam size and divergence cannot be neglected. For the majority of the photon energies the beam size and divergence are larger in the horizontal than the vertical plane. Therefore, the required kick to achieve a certain separation is minimized by performing the kick in the vertical plane.

4. Betatron tune choice

4.1. KAC requirements

The kicker requirements can be relaxed by modifying the vertical betatron tune of the ring from the nominal 3.15 such that only kicks of equal angle and polarity are required by the KAC scheme. This is achieved by finding a combination of tune and kicks where the orbit is restored within a few turns [6]. In this paper, the focus lies on schemes minimizing the number of required kicks since a large number of kicks makes the scheme more sensitive to the stability of the kicker [6]. A KAC scheme can be described as a superposition of the electron orbit for a series of kicks, where, in order to restore the orbit, the superposition for all kicks has to be zero [32]. For two kicks this results in the tune requirement $iQ = 0.5 + m$, where i is the number of turns between kicks and m an integer. The number of turns in a KAC cycle and the resulting required kick frequency for different solutions utilizing two kicks can be found in Table 3.

Table 3
Turns between kicks, resulting tune choice and required kick frequency.

Turns between kicks	Fractional tune	Kick frequency
1	0.5	3.125 MHz
2	0.25, 0.75	1.563 MHz
3	$\frac{1}{6} \approx 0.167$, 0.5, $\frac{5}{6} \approx 0.833$	1.042 MHz
4	0.125, 0.357, 0.625, 0.875	0.781 MHz
5	0.1, 0.3, 0.5, 0.7, 0.9	0.625 MHz

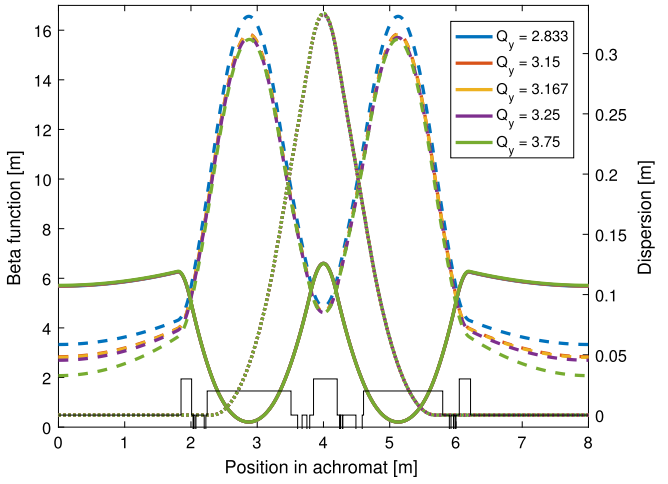

Fig. 2. Beta functions, horizontal (solid) and vertical (dashed), and dispersion (dotted) for lattices with vertical tune 2.833, 3.15 (nominal), 3.167, 3.25 and 3.75, respectively.

The nominal lattice of the MAX IV 1.5 GeV storage ring was modified to the desired vertical tunes using OPA [33]. Sufficient optimization was considered achieved when reaching the desired vertical tune without major changes to the optical functions. The resulting optical functions for different vertical tunes are displayed in Fig. 2. The changes are only negligible for the vertical tunes 3.167 and 3.25, and therefore these choices were considered preferable for operation in the real machine. The tune change required modification of the quadrupole gradient in the combined quadrupole–sextupole magnet family SQFi, and therefore resulted in a modification of the corresponding sextupole gradient. Since this magnet family is chromatic, the gradient modification had to be compensated by the chromatic sextupole magnets SCi and SDi to restore the nominal +1 chromaticity in both transverse planes. Studies of the dynamic aperture and Touschek lifetime with these modifications were performed using Tracy [34] with and without errors. The same error models were utilized as during the design studies of the ring [23]. The studies showed no reduction of dynamic aperture affecting injection and only a change of Touschek lifetime on the level of ±0.2%. Therefore, both lattices are considered to be feasible for operation in the real machine.

4.2. Optimization for beamlines

The choice of tune is also of importance to optimize the feasibility of the PSB mode in as many beamlines as possible. The electron beam orbit at a position s_2 when applying a kick θ at a position s_1 upstreams

[3] In this calculation the approximation

$$\sigma_r = \frac{\sqrt{2\lambda L}}{2\pi} \qquad \sigma_r' = \sqrt{\frac{\lambda}{2L}}, \tag{8}$$

where λ is the photon wavelength and L the undulator length [29] was used for the diffraction contribution to the convoluted beam since this is in better agreement for undulator radiation [25,30] than the commonly used approximation [31].

is given by

$$u(s_2) = \sqrt{\beta_{s_2}\beta_{s_1}}\sin(\Delta\Psi)\,\theta \tag{9}$$

$$u'(s_2) = \sqrt{\frac{\beta_{s_1}}{\beta_{s_2}}}\left(\cos(\Delta\Psi) - \alpha_{s_2}\sin(\Delta\Psi)\right)\theta, \tag{10}$$

where $\Delta\Psi$ is the phase advance between s_1 and s_2 [35]. For the simplest design of a PSB mode, the kicker and the source points of the beamlines are placed in the middle of the straight sections. For the MAX IV 1.5 GeV storage ring this gives $\alpha_{\text{kick}} = \alpha_{s_n} = 0$ and $\beta_{\text{kick}} = \beta_{s_n} = \beta$, where α_{s_n} and β_{s_n} are the Twiss parameters at the positions of the beamlines, and α_{kick} and β_{kick} the Twiss parameters at the position of the kicker. This gives the electron beam orbit at the beamline positions

$$u(s_n) = \theta\beta\sin\left(\Delta\Psi_{s_n}\right) \tag{11}$$

$$u'(s_n) = \theta\cos\left(\Delta\Psi_{s_n}\right), \tag{12}$$

where $\Delta\Psi_{s_n}$ is the phase advance between the kicker and the corresponding beamline. Since the phase advance of the MAX IV 1.5 GeV storage ring bare lattice is equal for each achromat, it is given by

$$\Delta\Psi_{s_n} = 2\pi n\frac{Q}{N_{\text{achr}}} = 2\pi n\Delta\Psi_{\text{achr}}, \tag{13}$$

where n is an integer describing how many achromats away the beamline is from the kicker and N_{achr} the total number of achromats. The phase advance per achromat is denoted by $\Delta\Psi_{\text{achr}}$. To evaluate the separation at different beamlines, a transfer function T describing the transfer between the applied kick and the resulting separation was defined as

$$S = T\theta. \tag{14}$$

For beamlines with an intermediate focus, the focused transfer function T_{f} was defined as

$$S = T_{\text{f}}\theta, \tag{15}$$

with

$$T_{\text{f}} = \frac{N_{\text{f}}\sigma_0}{\theta} = \beta\sin\left(2\pi\Delta\Psi_{\text{achr}}n\right), \tag{16}$$

where the sine function has the frequency $\Delta\Psi_{\text{achr}}$ and is sampled in the points n. Similarly, for beamlines without intermediate focus, the unfocused transfer function T_{uf} was defined as

$$S = T_{\text{uf}}d\theta \tag{17}$$

with

$$T_{\text{uf}} = \frac{N_{\text{uf}}\sigma_0'}{\theta} = \frac{\beta\sin\left(2\pi\Delta\Psi_{\text{achr}}n\right)}{d} + \cos\left(2\pi\Delta\Psi_{\text{achr}}n\right). \tag{18}$$

Note that the definition of the unfocused transfer function was made such that the influence of the distance from the source easily could be evaluated. It is apparent that the influence of the electron beam position depends on the ratio between the beta function and the distance to the source. Due to these definitions, the focused transfer function has the unit of length whereas the unfocused transfer function is unitless.

The two lattice candidates were evaluated for each beamline position over all n turns by the merit functions

$$M_A = \max_{1\le i\le n}\left(|T_i|\right), \tag{19}$$

which describes the maximum of the absolute transfer function over all turns, and

$$M_B = |T_{max} - T_{max-1}|, \tag{20}$$

which describes the absolute difference between the transfer functions of the turn with maximum transfer and the turn closest to it. The focused and unfocused M_A are displayed in Fig. 3. For unfocused separation the

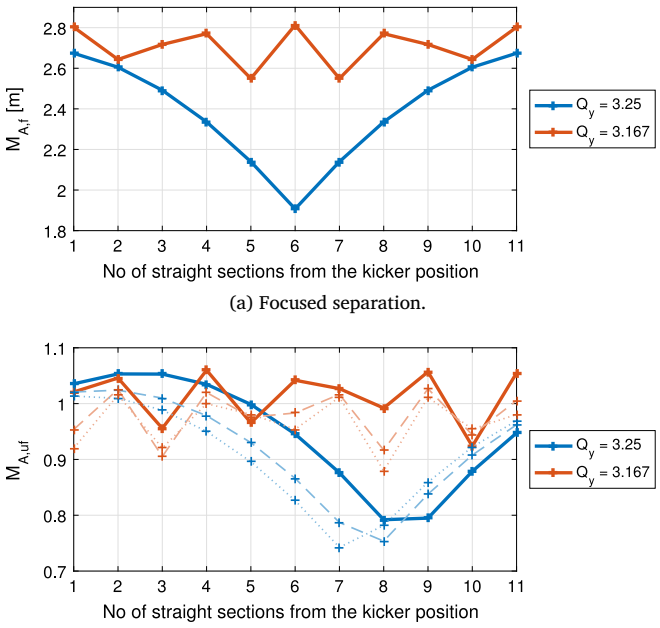

(a) Focused separation.

(b) Unfocused separation for a distance 8 m (solid), 12 m (dashed) and 16 m (dotted) from the source. The distances corresponds to positions where light separation is possible in the present MAX IV 1.5 GeV ring beamlines.

Fig. 3. The merit function M_A for the two vertical tune choices.

merit functions depend on the distance to the source so separation could be preferred at different distances depending on the beamline position. Studying the M_A, the vertical tune 3.167 is more promising than 3.25 for maximizing the separation in as many beamlines as possible for both focused and unfocused separation. This is because the PSB makes more turns before kicked back, and thus the probability increases for having at least one turn with sufficient value of the transfer function at every beamline. For a given M_A, the required kick to achieve a certain focused or unfocused separation can be dimensioned according to

$$\theta_{\text{f}} = \frac{N_{\text{f}}\sigma_0}{M_{A,\text{f}}} \tag{21}$$

$$\theta_{\text{uf}} = \frac{N_{\text{uf}}\sigma_0'}{M_{A,\text{uf}}}. \tag{22}$$

If the kick, for example, is dimensioned for $M_{A,\text{f}} = 2.5$ m or $M_{A,\text{uf}} = 1$, the resulting required kick angles to achieve 10σ separation of the photon beams are presented in Table 4. This separation is chosen here as an example and is discussed in more detail in Section 7. It can be noted that the ratio between the required kick angles are given by

$$\frac{\theta_{\text{f}}}{\theta_{\text{uf}}} = \frac{M_{A,\text{f}}}{M_{A,\text{uf}}}\frac{\sigma_0}{\sigma_0'} \approx \frac{1}{2.5}\frac{\sigma_0}{\sigma_0'}. \tag{23}$$

Since $\frac{\sigma_0}{\sigma_0'} < 2.5$ in the vertical plane for the whole photon energy range of interest, focused separation is more effective than unfocused separation for reducing the required kick. This results from the magnitude of the beta function in combination with the diffraction contribution to the photon beam size and divergence. Generally, for a diffraction-limited beam according to Eq. (8)

$$\frac{\sigma_0}{\sigma_0'} \approx \frac{\sigma_r}{\sigma_r'} = \frac{L}{\pi}, \tag{24}$$

where L is the undulator length, which is often smaller than the beta function in the straight section.

The M_B for several vertical tune choices are displayed in Fig. 4. More turns before the PSB is kicked back increases the difficulty to separate the radiation emitted from different turns, and thus leads to

Table 4
Estimated required kick to achieve 10σ separation in the vertical plane for $M_{A,\mathrm{f}} = 2.5$ m and $M_{A,\mathrm{uf}} = 1$, respectively.

Photon energy	Focused	Unfocused
40 eV	148 μrad	789 μrad
200 eV	123 μrad	355 μrad
1000 eV	72 μrad	164 μrad

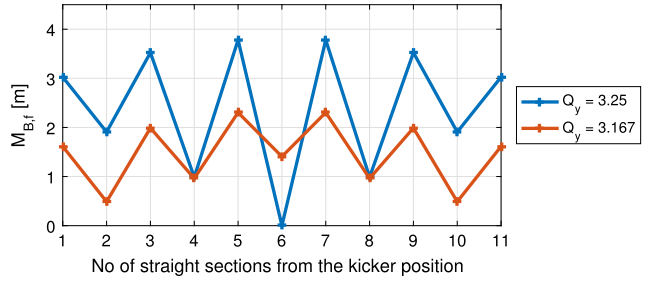

(a) Focused separation.

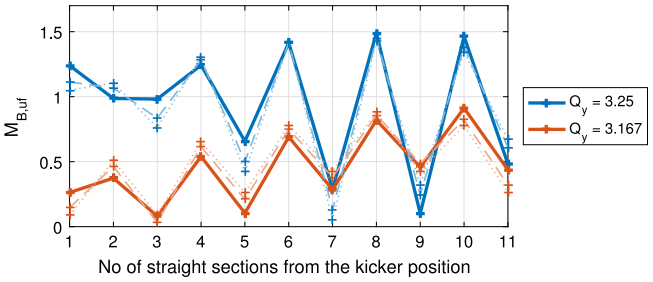

(b) Unfocused separation for a distance 8 m (solid), 12 m (dashed) and 16 m (dotted) from the source. The distances corresponds to positions where light separation is possible in the present MAX IV 1.5 GeV ring beamlines.

Fig. 4. The merit function M_B for the two vertical tune choices.

a smaller M_B. This can cause problems for some experiments since not only light from the turn with largest separation from the multibunch train will be seen by the beamline, but also some of the light produced by the PSB during other turns. Comparing the M_B values it is evident that overlapping of light from different PSB turns is a larger concern for unfocused than for focused separation, but it is a problem for some beamlines in both cases. It can, however, be solved by requiring choppers in the beamlines that wish to utilize the PSB mode. By setting this requirement it is possible to choose a PSB mode operated at the vertical tune 3.167 instead of 3.25, which gives large separation in all beamlines.

5. Electron beam orbit

The PSB electron orbit when applying a series of kicks was simulated with DIMAD [36] and compared to simulations performed with Accelerator Toolbox [37]. The two codes showed consistent results. The electron orbit for the kicks in Table 4 for a vertical tune of 3.167 are displayed in Fig. 5. The chosen kicks lead to maximum electron orbits between 0.48 and 0.99 mm for focused separation compared to 1.1–5.2 mm for unfocused separation. Presently the orbit limitations for machine protection are set to ±0.5 mm [38], but the studies behind this limitation did not consider a certain fill pattern so the effects from irradiating parts of the vacuum chamber have to be further analyzed to determine requirements for a PSB mode.

Simulations of several KAC cycles were performed in Accelerator Toolbox with cavity and radiation effects. The simulations were performed using the *atfastring* function for a lattice with and without

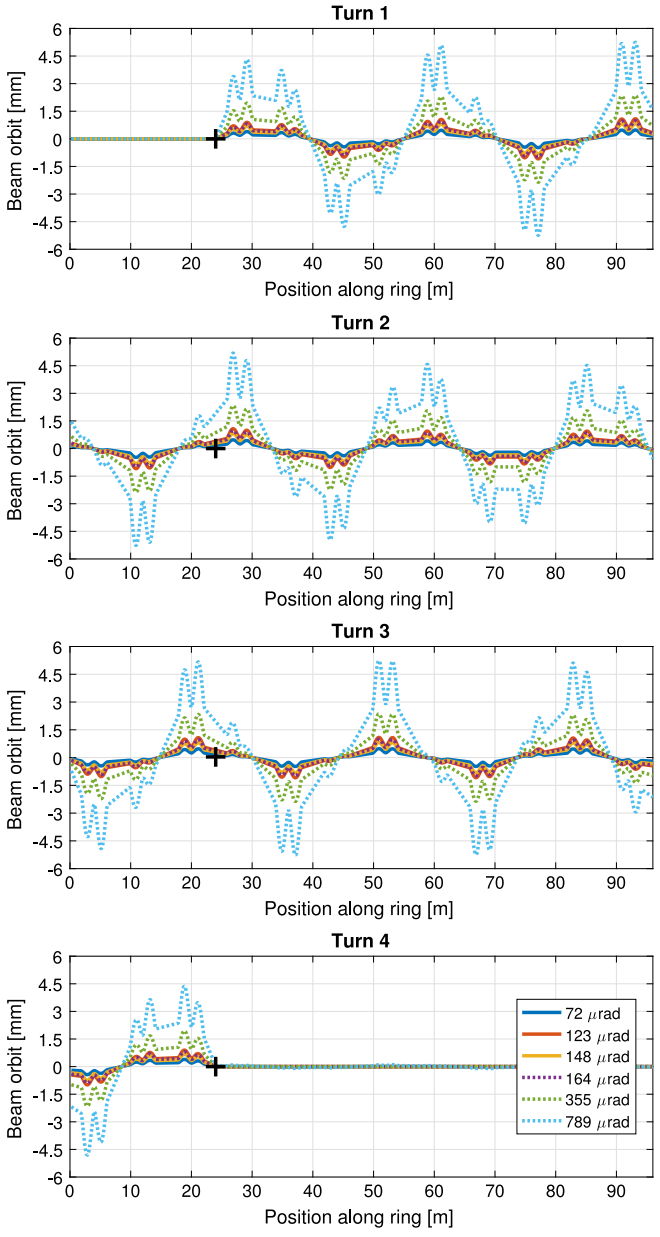

Fig. 5. Electron beam orbit for a vertical tune of 3.167 for different kicks simulated with DIMAD. The required orbits for focused separation according to the kicks in Table 4 are marked as solid whereas the orbits corresponding to unfocused separation are dotted.

PSB kick which allowed tracking for several damping times including quantum diffusion [39]. The lattice without PSB kick were first tracked for 60 000 turns to reach nominal values for beam size, energy spread, bunch length and emittance. The lattice was then tracked with or without PSB kick according to a given KAC scheme. As previously mentioned, a KAC scheme allows for variation of the PSB frequency, but due to resonances it is not feasible to operate at all frequencies [7]. If the KAC period is N (meaning the KAC cycle repeats every Nth turn), the PSB frequency becomes

$$f_{\mathrm{PSB}} = \frac{f_{\mathrm{rev}}}{N}, \tag{25}$$

where f_{rev} is the revolution frequency. Resonances causing unstable orbits occur when [7]

$$NQ = k, \tag{26}$$

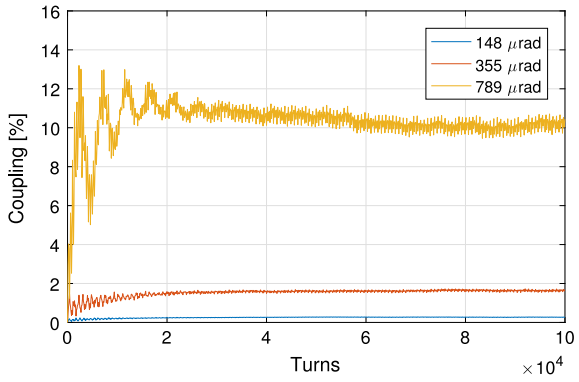

Fig. 6. Coupling increase due to vertical kicks at high frequency for different kicks. In the simulations 10 000 particles and a KAC scheme with $N = 7$ were used. The results every 100th turn are plotted.

where k is an integer, and at the coupling resonances

$$m_x(NQ_x) + m_y(NQ_y) = k. \tag{27}$$

For the coupling resonances the orbit can be stabilized by adjusting the horizontal tune [7], but this is not possible for the integer resonances. For a vertical tune of 3.167, assuming a maximum available kick frequency according to Table 3, the maximum stable PSB frequency is at $N = 7$ corresponding to 446 kHz. It would also be possible to operate at $N = 4$ or $N = 5$, but this requires a kicker that can kick with higher frequency than required by the tune choice. The simulations showed that the orbit becomes unstable at the resonances predicted by theory.

If the PSB is not at the correct betatron tune, an orbit deviation will remain after a KAC cycle, which after several cycles translates into a stable oscillation of the bunch. The design specifications of the ring allow for oscillation of the electron beam centroid up to 10% of the electron beam size [14], corresponding to 1.3 μm in the vertical plane. It is however likely that the requirement on maximum electron beam oscillation can be relaxed since the PSB is only one of 32 bunches for the multibunch users, and since the timing users are mostly interested in photon energies where the photon beam size is dominated by diffraction and thus substantially larger than the electron beam size. The lattice optimization was performed to put the working point at the correct vertical tune to simulate the effect of operating the multibunches on a resonance, which resulted in a small tune deviation for the PSB due to chromatic and amplitude-dependent tune shifts. The effect of this was simulated and it was found that it could be compensated by a small modification of the working point such that the tune of the PSB becomes correct including the nonlinear tune shifts.

In addition, the coupling increase caused by the PSB going off-axis through the sextupoles and kicking the beam at high frequency was evaluated by studying the increase of the vertical emittance. For the ideal, uncoupled lattice the vertical emittance at the initial equilibrium was zero but, as displayed in Fig. 6, a new equilibrium is reached when running KAC. The coupling increase for a 789 μrad kick for the maximum stable PSB frequency $N = 7$ is considered to large for operation, but for a 355 μrad kick the increase is below 2%, which is considered acceptable. The coupling increase is, however, dependent on the PSB frequency and becomes smaller further away from resonances.

In the ring tune deviations occur due to insertion device gap motion and power supply jitter and the tune has to be sufficiently stable not to give rise to too large PSB oscillations. The residual orbit amplitude after a KAC cycle is given by

$$\Delta u \approx 2\pi\theta\beta\Delta n\Delta Q, \tag{28}$$

where Δn is the number of turns before the beam is kicked back. For the vertical tune 3.167 and the kicks in Table 4 this gives maximum

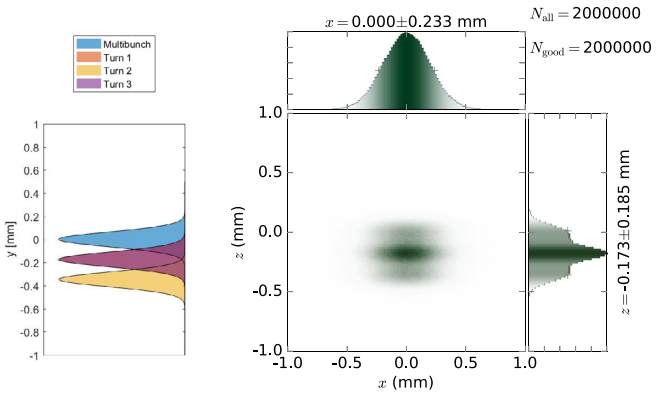

(a) Photon energy 40 eV. Separation to multibunch: 4.49 FWHM/2. Separation to closest PSB: 2.25 FWHM/2.

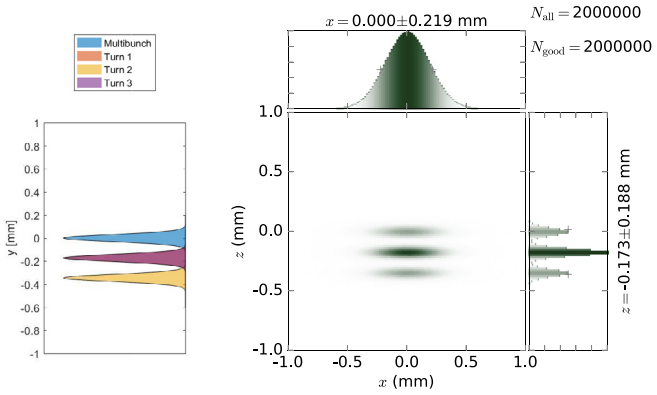

(b) Photon energy 200 eV. Separation to multibunch: 10.18 FWHM/2. Separation to closest PSB: 5.09 FWHM/2.

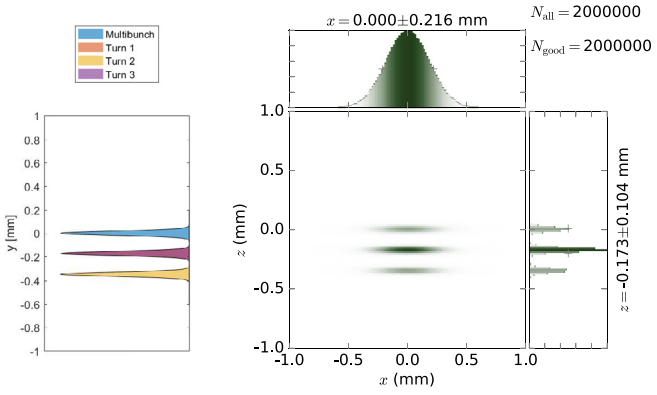

(c) Photon energy 1000 eV. Separation to multibunch: 15.73 FWHM/2. Separation to closest PSB: 7.86 FWHM/2.

Fig. 7. XRT simulations for a vertical tune of 3.167 for different photon energies at the source. In this example 123 μrad kick and a beamline position six achromats from the kicker were used. The photon energy ranges were set to 0.1%BW.

allowed tune variations between $1.7 - 3.4 \cdot 10^{-4}$ for focused separation and $1.5 - 3.1 \cdot 10^{-5}$ for unfocused separation.

6. Beamline simulations

The output from the simulations of the electron beam orbit was used to simulate the photon beam separation for undulator radiation using XRT [40]. For these simulations, an example undulator with period length 59.5 mm, total length 2.5 m and a maximum K value of 6 was

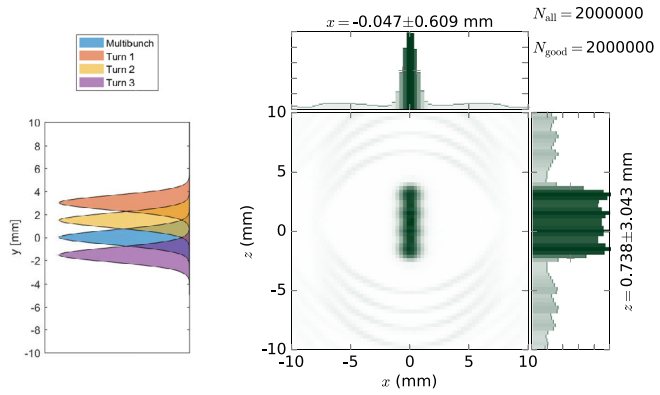

(a) Photon energy 40 eV. Separation to multibunch: 4.11 FWHM/2. Separation to closest PSB: 2.09 FWHM/2.

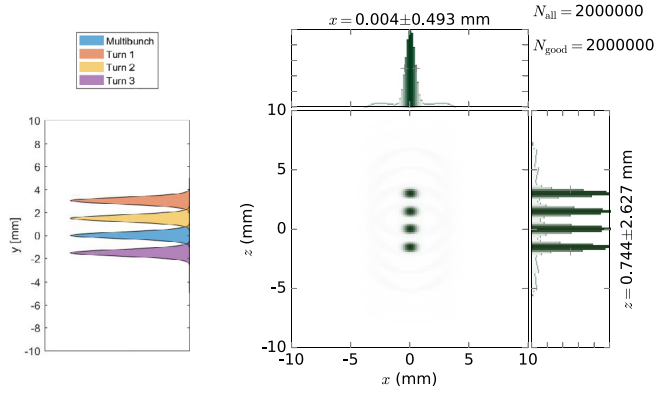

(b) Photon energy 200 eV. Separation to multibunch: 9.54 FWHM/2. Separation to closest PSB: 4.85 FWHM/2.

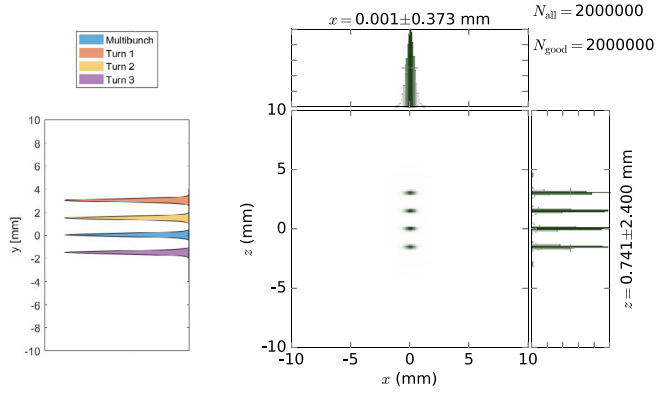

(c) Photon energy 1000 eV. Separation to multibunch: 19.94 FWHM/2. Separation to closest PSB: 10.13 FWHM/2.

Fig. 8. XRT simulations for a vertical tune of 3.167 for different photon energies at a screen 8 m from the source. In this example 355 μrad kick and a beamline position four achromats from the kicker was used. The photon energy ranges were set to 0.1%BW.

used. The parameters were chosen to represent a common undulator in the MAX IV 1.5 GeV storage ring. For this undulator, 40 eV and 200 eV are first harmonics whereas 1000 eV is a third harmonic. Since undulator radiation is not Gaussian, the beam size was described by $\frac{\text{FWHM}}{2} = \sqrt{2 \ln 2}\sigma \approx 1.18\sigma$ since this resulted in a better measure of the size of the central peak of the radiation. For focused separation it is the separation at the source that is of interest since this will be imaged onto the plane where the separation is performed, whereas for unfocused separation the separation 8 m from the source was studied since this is

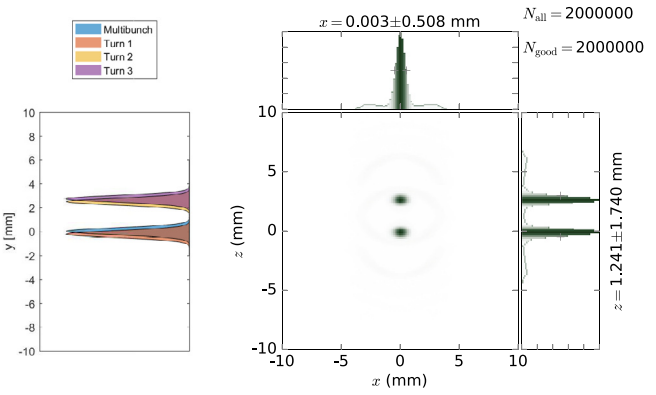

(a) Vertical tune 3.167.

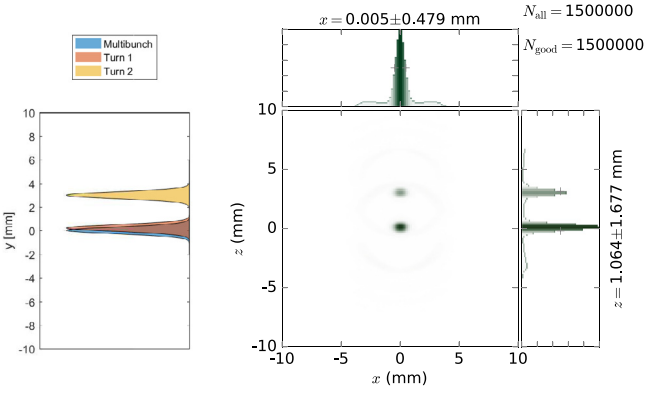

(b) Vertical tune 3.25.

Fig. 9. XRT simulations for a vertical tune of 3.167 (top) and 3.25 (bottom) at a screen 8 m from the source. In this example 355 μrad kick, 200 eV photon energy and a beamline position three achromats from the kicker were used.

the position in the present MAX IV 1.5 GeV ring beamlines which would result in largest M_A for most beamlines.

For a kick of 123 μrad (dimensioned to achieve 10σ separation at 200 eV photon energy for focused separation) a comparison for different photon energies at the source is displayed in Fig. 7. A similar comparison for 355 μrad kick (dimensioned to achieve 10σ separation at 200 eV photon energy for unfocused separation) at 8 m from the source is displayed in Fig. 8. It is evident that for photon energies below 200 eV, which the kick is dimensioned for, the maximum separation is reduced for both focused and unfocused separation, whereas for higher photon energies it is increased.

As discussed earlier, overlap between the light from different PSB turns can occur if the M_B value is too small. Fig. 9 displays a comparison for a beamline position three achromats from the kicker that utilizes unfocused separation. At this position, overlap between PSB turns occurs for the vertical tune 3.167, but not for 3.25, as expected considering the M_B values. The XRT simulation displays the situation as seen when integrating over time, thus the radiation from different PSB turns in this case cannot be separated without a chopper in the beamline.

7. Purity

For the users, the purity between the light from the PSB and the light from the rest of the multibunch train is of great importance. In this paper the purity is defined as the ratio between the light from the PSB and one of the multibunch bunches. Since the principle of the PSB method is to place an aperture such that the radiation emitted from the multibunches is blocked, the purity will depend on the size of the aperture. Therefore, for a given separation the flux and purity

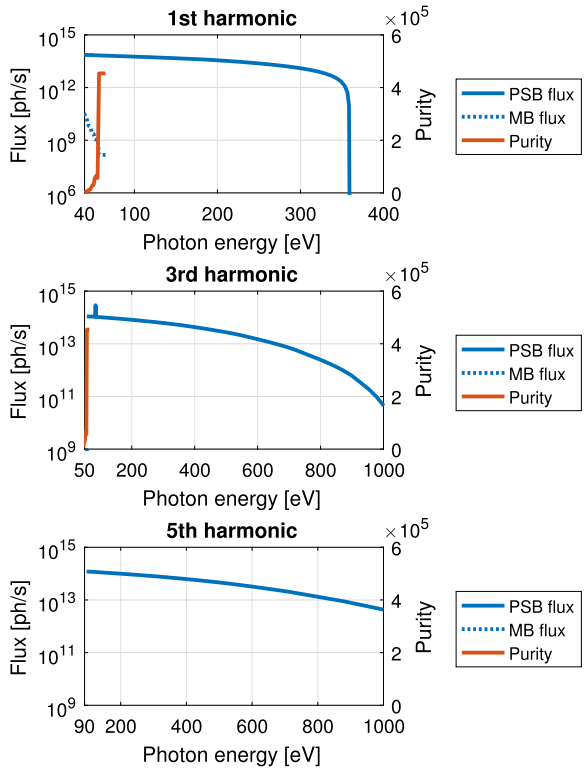

Fig. 10. Purity tuning curves calculated with XRT for a vertical tune of 3.167, 123 μrad kick and focused separation for a $\pm 2\sigma \times \pm 2\sigma$ slit. In this example a beamline position six achromats from the kicker was used. In the simulations 500 000 rays were used and the photon energy ranges set to 0.1%BW. For the energy ranges where no purity is presented the flux through the slit from a multibunch was calculated to be zero.

can to some extent be optimized according to the requirements of the experiments by modifying the aperture size to sacrifice flux for purity and vice versa.

To study the purity as function of photon energy for a given kick, XRT simulations were performed with the example undulator described in the previous section for two different example beamlines, one utilizing focused separation where the source is imaged onto a slit placed 16 m from the source by a mirror placed 8 m from the source, and one utilizing unfocused separation with a slit placed 8 m from the source. Fig. 10 displays the purity for focused separation, whereas the corresponding purity for unfocused separation is displayed in Fig. 11. In both cases the size of the slit was chosen as a trade off between purity and flux. Despite similar separation from the multibunch train, the purity is substantially smaller for unfocused than focused separation. The reason for this lies in the properties of the angular beam profile of undulator radiation. For unfocused separation, the photon beam profile at the separation point will be dominated by the angular beam profile of the source. For a certain photon energy, in addition to a central peak, radiation is also emitted in a ring pattern around the central peak due to radiation from higher harmonics being shifted to lower frequency at large angles [41]. This ring pattern can be recognized in the beam profiles presented in Fig. 8. It is evident that the ring pattern caused by the angular beam profile can seriously reduce the purity if the kick is such that the PSB will be situated at the same angle as the rings produced by the multibunches.

Fig. 12 displays the purity for focused and unfocused separation as function of electron beam position and angle at the source, respectively. Depending on exact user requirements, for focused separation sufficient purity could possibly be achieved below the 10σ separation used as an example in this paper. For unfocused separation, however, substantial purity increase can only be achieved if the PSB is kicked beyond the strongest rings. The angular position of the rings are given by [41]

$$\theta_{n,l} = \frac{1}{\gamma}\left[\frac{l}{n}\left(1+\frac{K^2}{2}\right)\right]^{1/2}, \tag{29}$$

where n is the harmonic, $l = 1, 2, 3\ldots$ and K the undulator parameter. Applying the on-axis undulator equation $\lambda = \frac{\lambda_u}{2\gamma^2 n}\left(1+\frac{K^2}{2}\right)$ [41], this can be written as

$$\theta_{n,l} = \sqrt{\frac{2l}{\lambda_u}\lambda}, \tag{30}$$

where λ_u is the undulator period. The wavelength is connected to the PSB kick by Eq. (22) and (8) as

$$\theta_{\mathrm{uf}} \approx N_{\mathrm{uf}}\sigma_0' \approx N_{\mathrm{uf}}\sigma_r' = N_{\mathrm{uf}}\sqrt{\frac{\lambda}{2L}}, \tag{31}$$

resulting in

$$\theta_{n,l} = \sqrt{\frac{4lL}{\lambda_u}}\frac{\theta_{\mathrm{uf}}}{N_{\mathrm{uf}}}. \tag{32}$$

A kick beyond a ring requires $\theta_{n,l} < \theta_{\mathrm{uf}}$, which leads to the requirement

$$N_{\mathrm{uf}} > \sqrt{\frac{4lL}{\lambda_u}}, \tag{33}$$

and a separation above 10σ as found in Fig. 12.

From the purity, the integrated purity that will be seen by a beamline which integrates over time can be calculated for a given charge distribution in the ring, KAC operation scheme and beamline configuration by calculating the number of multibunches per PSB and taking into account the charge distribution among the buckets. If the purity for nominal charge per bunch is P, the integrated purity is given by

$$P_{\mathrm{int}} = \frac{q_{\mathrm{rel}}P}{N_{\mathrm{MB}}}, \tag{34}$$

where q_{rel} is the relative charge in the PSB compared to the nominal charge in the multibunches and N_{MB} the number of multibunches seen by the beamline per PSB. In the case of no chopper in the beamline, the number of multibunches per PSB will depend on the period between KAC cycles. Avoiding periods between cycles that lead to resonances and assuming the maximum frequency of the kicker is given by the required frequency for KAC in Table 3, the maximum frequency with which a PSB could be seen in a beamline is, in accordance with the discussion in Section 5,

$$f_{\mathrm{PSB}} = \frac{f_{\mathrm{rev}}}{2i+1}, \tag{35}$$

where f_{rev} is the revolution frequency and i the number of turns between kicks in the KAC cycle. The number of multibunches seen by the beamline during a PSB period (if the PSB during turns not used by the beamline are counted as multibunches) is

$$N_{\mathrm{MB}} = h\frac{f_{\mathrm{rev}}}{f_{\mathrm{PSB}}} - 1 = hN - 1, \tag{36}$$

where h is the harmonic number of the ring and N the number of turns before the KAC scheme repeats. On the other hand, with a chopper in the beamline the number of multibunches are given by the chopper window. The number of multibunches seen by the beamline is then

$$N_{\mathrm{MB,\ chopper}} = \Delta t f_{\mathrm{rev}} h - 1, \tag{37}$$

where Δt is the time duration of the chopper window. As displayed in Fig. 13, the integrated purity increases linearly with the PSB frequency and proportionally to the relative charge in the PSB compared to the multibunches. However, when using a chopper the integrated purity is given by the length of the window and is no longer dependent on the PSB frequency.

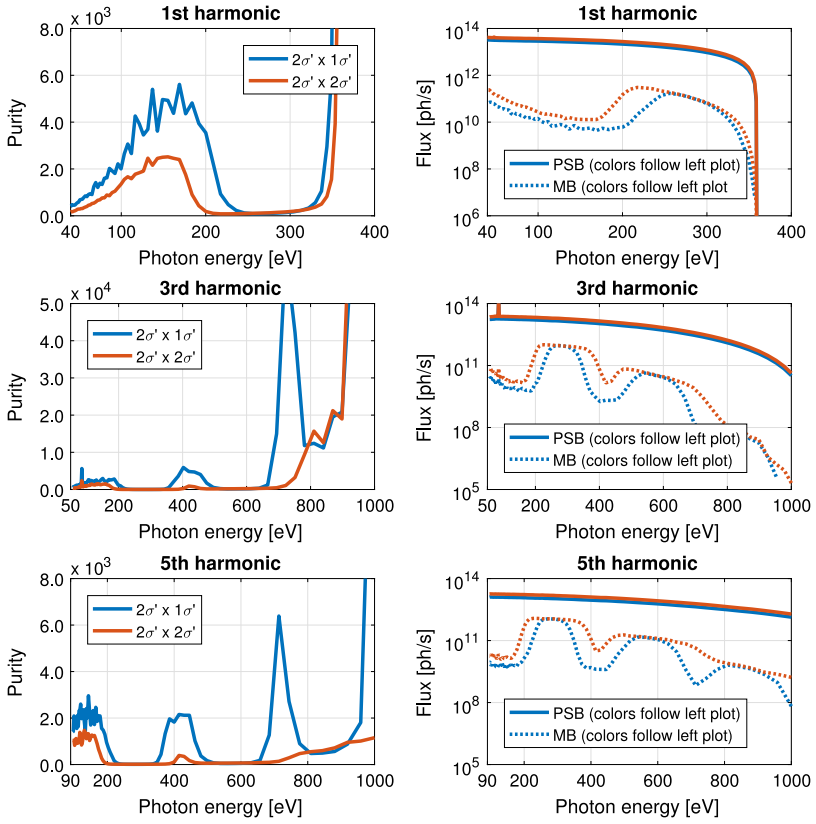

Fig. 11. Purity tuning curves calculated with XRT for a vertical tune of 3.167, 355 μrad kick and unfocused separation at a distance 8 m from the source for two different slit sizes. In this example a beamline position four achromats from the kicker was used. In the simulations 500 000 rays were used and the photon energy ranges set to 0.1%BW.

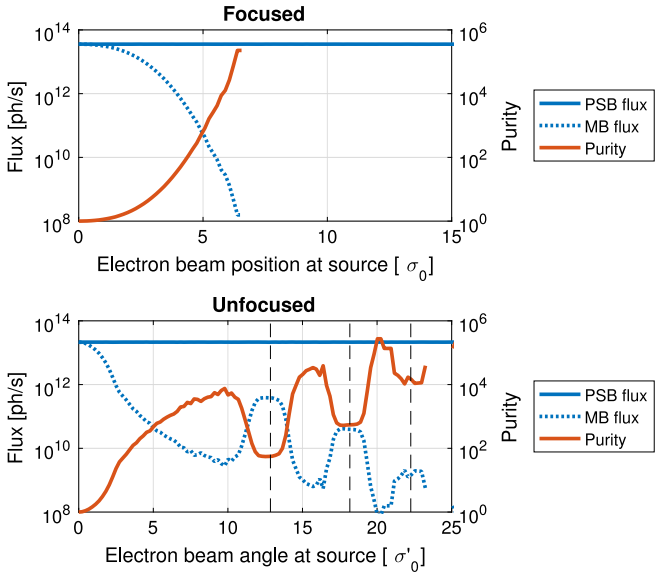

Fig. 12. Purity for focused and unfocused separation as function of electron beam position and angle at the source in units of photon beam size and beam divergence at the source, respectively. In this example a first harmonic 200 eV photon energy was used. The dashed lines mark the theoretical positions of the rings in the angular beam profile. In the simulations 500 000 rays were used, the photon energy ranges set to 0.1%BW and the slit sizes to $\pm 2\sigma \times \pm 2\sigma$ and $\pm 2\sigma \times \pm 1\sigma$, respectively. For the energy ranges where no purity is presented the flux through the slit from a multibunch was calculated to be zero.

8. Kicker requirements

The ALS PSB mode utilizes a stripline kicker for deflecting the PSB transversely [42], and a similar design is considered for a PSB mode at the MAX IV 1.5 GeV storage ring. For this kicker, three parameters are set by the PSB mode design: pulse length, repetition rate and kick amplitude. Since the aim of the development of PSB modes at the MAX IV rings is to serve timing users without requiring gaps in the multibunch fill, the pulse length is critical and determined by the interval between bunches in the multibunch train, resulting in a rise/fall time of < 10 ns and a maximum total pulse length of ≤ 20 ns. The maximum repetition rate is set by the tune choice or the maximum PSB frequency that should be available for users if this is higher than determined by the tune. Finally, the required kick is determined by the purity requirements of the users.

The maximum pulse length sets a limit on the maximum length of a stripline since the propagation time of the pulse along the stripline and the bunch length also has to be taken into account. The maximum length is given by

$$L \leq \frac{\tau_G - \tau_R - \tau_b}{2} c, \tag{38}$$

where τ_G is the gap between adjacent bunches, τ_R the rise/fall time of the pulse and τ_b the bunch length [43]. The profile of a lengthened bunch in the MAX IV 1.5 GeV storage has a full width of roughly 1.3 ns, which, with 10 ns spacing between bunches, leads to a maximum rise time of 6.7 ns for a 0.3 m kicker, 4.7 ns for a 0.6 m kicker, or 2.0 ns for a 1 m kicker.

The kick requirement determines the necessary voltage on each stripline according to

$$\pm V = \frac{E \cdot h \cdot \theta}{4 \cdot L \cdot g}, \tag{39}$$

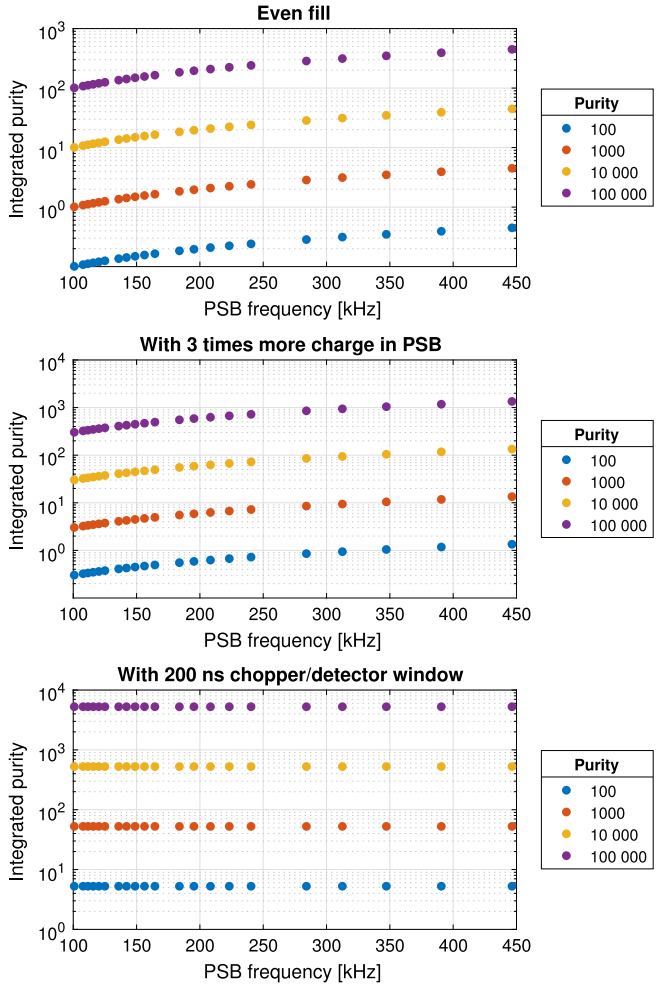

Fig. 13. Estimated integrated purity for given values of purity as a function of stable frequencies for even fill, a fill with 3 times more charge in the PSB and even fill with a 200 ns chopper window. Here, a KAC mode with 3 turns in a cycle was used.

where E is the beam energy in eV, h the transverse distance between the striplines, θ the kick, L the length of a stripline, and g a geometry factor [42]. Since the length of a stripline is a factor in Eq. (39), the voltage and pulse length are not independent. It is possible to decrease the voltage requirement by placing several stripline modules after one another (thus increasing the total length without requiring shorter rise/fall time). This, however, means the kicker will occupy more space in the ring (due to required spacing between modules), in addition to requiring several pulsers [44], which have to be synchronized to a high degree in order to preserve the PSB beam quality.

The kicker specifications for some different designs can be found in Fig. 14. A geometry factor between 0.95 and 1 is expected to be feasible. In these calculations, 20 mm spacing vertically have been used in accordance with the nominal vacuum chamber dimensions in the straight sections of the MAX IV 1.5 GeV storage ring [14].

The required kicker stability can be estimated from the orbit amplitude at the beginning of a new KAC cycle caused by the residual kick from the previous KAC cycle. This is given by

$$\Delta u = \Delta\theta\beta \sin(2\pi Q), \tag{40}$$

where $\Delta\theta$ is the difference in kick between the two kicks in the KAC cycle. The maximum kick difference is then 0.53 μrad for a vertical tune of 3.167 and a electron beam oscillation limit of 1.3 μm. Using equation

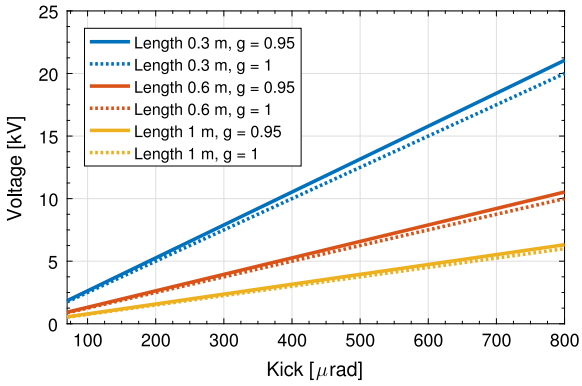

Fig. 14. The required voltage to achieve a certain kick for various stripline specifications.

(39), this can be translated to a voltage stability on the kicker power supply as

$$\frac{\Delta V}{V} = \frac{\Delta\theta}{\theta}, \tag{41}$$

which leads to a maximum allowed voltage jitter of 0.43% for a 123 μrad kick and 0.15% for a 355 μrad kick before the residual amplitude at the beginning of a new KAC cycle caused by the residual kick from the previous KAC cycle becomes greater than the 1.3 μm limit.

9. Local orbit bumps

As mentioned previously, to be able to quickly switch between PSB and multibunch operation without realigning the beamline and to conserve the polarization properties of the emitted radiation, local orbit bumps that put the PSB on axis through the straight sections are required. In the MAX IV 1.5 GeV storage ring lattice, dipole correctors are formed by individually powered extra windings on some of the sextupole magnets. The correctors have been designed to supply 0.25 mrad kick [14].

The required corrector strength was calculated both analytically and with SVD using response matrices in Accelerator Toolbox with consistent results. To put the PSB on-axis throughout a straight section, at least four correctors are required, but due to the positions of correctors and BPMs a four corrector bump will lead to a non-zero orbit in the arc BPM. For a 355 μrad kick this orbit is below 80 μm. To force a zero orbit in the arc at least five correctors are required. The results show that the available corrector strength is not sufficient, but has to be increased depending on the chosen PSB kick. To achieve 10σ separation at 200 eV the peak corrector strength has to be increased by roughly a factor 2 for focused separation compared to 5–6 for unfocused separation depending on if the orbit is allowed to grow in the arcs or not. However, only the corrector strengths surrounding the straight sections that are interested in operating in PSB mode have to be increased.

10. Consequences for the MAX IV 1.5 GeV storage ring

None of the five current beamlines at the MAX IV 1.5 GeV storage ring has an intermediate focus [24–28] and therefore comparison with other methods are required to determine if a PSB mode is the best choice for increasing the available beamtime for timing users at these beamlines. However, as mentioned previously, space exists for five new beamlines and if these beamlines are designed with an intermediate focus a PSB mode can serve timing users at these beamlines with high purity while the ring is operated in multibunch mode without extensive machine upgrades. For this PSB mode three requirements are proposed:

- Kick performed in the vertical plane.

- Dimension the kick to achieve a given number of sigma separation at a given photon energy in all beamlines based on a trade off between user purity requirements and machine limitations.
- Choppers with a time window < 320 ns in all beamlines wishing to operate in PSB mode.

The purity requirements of the users remains to be fully determined. However, for the photon energy range of interest, diffraction substantially influences the machine requirements and it is not expected to be feasible to achieve sufficient purity for all users over the whole energy range 4–1500 eV. For the lowest photon energies a single-bunch mode or another method will still be required. The choice of kick magnitude therefore has to be a balance between user requirements and machine limitations. For focused separation the 10σ separation estimated in this article could possibly be reduced after more detailed studies of the purity including the quality and stability of the beamline optics. Beamline experiments will be required to obtain a better estimation of the purity and separation requirements. Presently, the beamlines at the MAX IV 1.5 GeV ring are under construction or commissioning, but such studies will follow once they come online. For unfocused separation, however, the purity is limited by the angular beam profile and a substantial gain in purity would require kicks that are beyond machine limitations. Once the purity requirements have been determined, further studies could be conducted to find undulator designs or operation modes that would improve the purity, but this might pose restrictions on the photon energy range or polarization.

Adding a chopper to the beamline offers several advantages. It will greatly improve the integrated purity and make it feasible for beamlines to choose their operation frequency independently of one another. The requirements for such choppers are similar to the requirements for choppers for operation in single-bunch mode and they could thus be utilized for operation in both modes. In addition, by requiring a chopper in each beamline that wishes to utilize the PSB mode, it will be possible to choose a mode operated at a vertical tune of 3.167 despite the overlap of radiation from different PSB turns. Compared to a vertical tune of 3.25, this gives high M_A in all beamlines. This choice also reduces the required repetition rate of the kicker to 1.04 MHz compared to 1.56 MHz for a 3.25 tune.

11. Conclusions

The studies presented in this paper highlight that machine requirements (i.e. kicker strength and stability, tune stability, coupling increase, corrector strength, and orbit limitations due to machine protection) for a PSB mode to achieve a certain purity are greatly reduced if the beamlines have an intermediate focus before the monochromator where the photon beams can be separated. This emphasizes the importance of studying both machine and beamline design in order to fully optimize the performance of a PSB mode, as well as other methods with the purpose of serving both high flux and timing users simultaneously. It is evident that a solution with optimal performance for users can only be achieved by a design that includes measures on both the machine and the beamline side.

The feasible photon energy range is bounded by machine limitations since the separation required to achieve sufficient purity at low energies are determined by diffraction. This is the case for all methods that aim to provide single-bunch light when operating a ring in multibunch mode by separating photon beams transversely. Since some timing users are interested in UV energies, transverse methods are not sufficient to serve the whole timing user community when simultaneously serving high-flux users at the same ring. For these photon energies, methods based on separation in longitudinal phase space might be more attractive and require further consideration. For example, methods where one bunch in the bunch train is off energy by tailoring the nonlinear momentum compaction and thus creating several stable energy points [45,46]. If sufficient energy deviation can be achieved, the light from different bunches could be separated by a monochromator in the beamline.

This paper presents the possibility to operate a PSB mode serving all beamlines with only a single kicker by adequately choosing the tune and requiring choppers in the beamlines. This reduces the required kick frequency and the position of the kicker can be chosen independently of the position of the beamlines interested in PSB operation. In addition, choppers allow beamlines to choose frequency independent of one another and greatly increase the integrated purity.

Acknowledgments

The authors wish to thank Noelle Walsh for fruitful discussions concerning the user requirements, as well as Christian Stråhlman and Stacey Sorensen for their input on this subject. Thanks to Konstantin Klementiev for updates of XRT and assistance with the code, as well as Alexei Preobrajenski, Reiner Pärna and Rami Sankari for their help with beamline requirements. Thanks also to David Olsson for assistance with determining kicker requirements and Hamed Tarawneh for input on undulator radiation theory. Finally, thanks to Sverker Werin and Åke Andersson for their advice regarding the manuscript.

References

[1] J.M. Byrd, S. De Santis, J. Jacob, V. Serriere, Phys. Rev. ST Accel. Beams 5 (2002) 092001.
[2] N. Milas, L. Stingelin, Impact of filling patterns on bunch length and lifetime at the SLS, in: Proceedings of International Particle Accelerator Conference, Kyoto, 2010, p. 4719, THPE084.
[3] G. Bassi, A. Blednykh, S. Krinsky, J. Rose, Self-consistent simulations of passive landau cavity, in: Proceedings of North American Particle Accelerator Conference, Pasadena, 2013, p. 177, MOPBA03.
[4] M. Borland, T. Berenc, R. Lindberg, A. Xiao, Tracking studies of a higher-harmonic bunch-lengthening cavity for the APS upgrade, in: Proceedings of International Particle Accelerator Conference, Richmond, 2015, p. 543, MOPMA007.
[5] J.M. Byrd, S. De Santis, T. Luo, C. Steier, Phase transients in the higher harmonic RF system for the ALS-U proposal, in: Proceedings of International Particle Accelerator Conference, Richmond, 2015, p. 3372, WEPTY044.
[6] C. Sun, G. Portmann, M. Hertlein, J. Kirz, D.S. Robin, Pseudo-single-bunch with adjustable frequency: A new operation mode for synchrotron light sources, Phys. Rev. Lett. 109 (2012) 264801.
[7] C. Sun, D.S. Robin, C. Steier, G. Portmann, Characterization of pseudosingle bunch kick-and-cancel operational mode, Phys. Rev. ST. Accel. Beams 18 (2015) 120702.
[8] M.P. Hertlein, A. Scholl, A.A. Cordones, J.H. Lee, K. Engelhorn, T.E. Glover, B. Barbrel, C. Sun, C. Steier, G. Portmann, D.S. Robin, X-rays only when you want them: optimized pump–probe experiments using pseudo-singlebunch operation, J. Synchrotron. Radiat. 22 (2015).
[9] L.S. Nadolski, J.-P. Lavieville, P. Lebasque, A. Nadji, J.-P. Ricaud, M. Silly, F. Sirotti, First measurements with a kicked off axis bunch for pseudo single bunch mode studies at SOLEIL, in: Proceedings of International Particle Accelerator Conference, San Sebastián, 2011, p. 2912, THPCOO5.
[10] K. Holldack, R. Ovsyannikov, P. Kuske, R. Müller, A. Schälicke, M. Scheer, M. Gorgoi, D. Kühn, T. Leitner, S. Svensson, N. Mårtensson, A. Föhlisch, Single bunch X-ray pulses on demand from a multi-bunch synchrotron radiation source, Nat. Commun. 5 (2014) 4010.
[11] M. Ries, J. Feikes, T. Goetsch, P. Goslawski, J. Li, M. Ruprecht, A. Schälicke, G. Wustefeld, Transverse resonance island buckets at the MLS and BESSY II, in: Proceedings of International Particle Accelerator Conference, Richmond, 2015, p. 138, MOPWA021.
[12] P. Goslawski, J. Feikes, K. Holldack, A. Jankowiak, R. Ovsyannikov, M. Ries, M. Ruprecht, A. Schälicke, G. Wüstefeld, Resonance island experiments at BESSY II for user applications, in: Proceedings of International Particle Accelerator, Busan, 2016, p. 3427, THPMR017.
[13] Å. Andersson, E. Elafiffi, M. Eriksson, D. Kumbaro, P. Lilja, L. Malmgren, R. Nilsson, H. Svensson, P.F. Tavares, J. Hottenbacher, A. Salom, A. Milan, The 100 MHz RF system for the MAX IV storage rings, in: Proceedings of International Particle Accelerator Conference, San Sebastián, 2011, p. 193, MOPC051.
[14] MAX IV Detailed Design Report (2010), available at https://www.maxiv.lu.se/publications/.
[15] S. Sorensen, N. Mårtensson, R. Feifel, C. Stråhlman, S. Leemann, Preliminary report on alternate bunch schemes for the MAX IV storage rings, 2014, available at: https://www.maxiv.lu.se/science/accelerator-physics/current-projects/timing-modes-for-the-max-iv-storage-rings/.
[16] N. Walsh, S. Sorensen, R. Feifel, M. Gisselbrecht, M. Huttula, K. Jänkäla, A. Kivimäki, R. Pärna, V. Pankratovs, C. Stråhlman, M. Tchaplyguine, J. Uhlig, S. Urpelainen, G Öhrwall, S.C. Leemann, T. Olsson, Science Case for Single-Bunch mode at the 1.5 GeV ring, 2016, summary available at: https://www.maxiv.lu.se/science/accelerator-physics/current-projects/timing-modes-for-the-max-iv-storage-rings/.

[17] P.F. Tavares, S.C. Leemann, M. Sjöström, Å. Andersson, J. Synchrotron. Radiat. 21 (2014) 862.
[18] C. Stråhlman, T. Olsson, S.C. Leemann, S.L. Sorensen, Preparing the MAX IV storage rings for timing-based experiments, in: AIP Conference Proceedings, Vol. 1741, 2016, p. 020043.
[19] C. Pappas, S. De Santis, J.-Y. Jung, T. Lou, C. Steier, C. Swenson, W. Waldron, Prototyping for ALS-U fast kickers, in: Proceedings of International Particle Accelerator Conference, Busan, 2016, p. 3637, THPMW038.
[20] F. Lenkszus, A. Xiao, J. Carwardine, A. Cours, G. Decker, L. Morrison, X. Sun, J. Wang, F. Westferro, C.Y. Yao, A. Krasnykh, Fast injection system R&D for the APS upgrade, in: Proceedings of International Particle Accelerator Conference, Richmond, 2015, p. 1797, TUPJE069.
[21] C.J. Bocchetta, M. Bartosik, P.P. Goryl, K. Królas, M. Młynarczyk, W. Soroka, M.J. Stankiewicz, P.S. Tracz, Ł. Walczak, A.I. Wawrzyniak, K. Wawrzyniak, J. Wiechecki, M. Zajac, L. Zytniak, R. Nietubyc, Overview of the solaris facility, in: Proceedings of International Particle Accelerator Conference, New Orleans, 2012, p. 1650, TUPPP019.
[22] S.C. Leemann, Phys. Rev. ST. Accel. Beams. 17 (2014) 050705.
[23] S.C. Leemann, Lattice design for the MAX IV storage rings, in: ICFA Beam Dynamics Newsletter No. 71, Editor J. Gao, August 2017, available at http://icfa-bd.kek.jp.
[24] A. Preobrajenski, Beamline manager FlexPES, private communication 2016.
[25] R. Pärna, R. Sankari, E. Kukk, E. Nõmmiste, M. Valden, M. Lastusaari, K. Kooser, K. Kokko, M. Hirsimäki, S. Urpelainen, P. Turunen, A. Kivimäki, V. Pankratov, L. Reisberg, F. Hennies, H. Tarawneh, R. Nyholm, M. Huttula, FinEstBeaMS - wide-range finnish-estonian beamline for materials science at the 1.5 GeV storage ring at the MAX IV laboratory, Numer. Instrum. Methods A 859 (2017) 83.
[26] S. Urpelainen, C. Såthe, W. Grizolli, M. Agåker, A.R. Head, M. Andersson, S.W. Huang, B.N. Jensen, E. Wallén, H. Tarawneh, R. Sankari, R. Nyholm, M. Lindberg, P. Sjöblom, N. Johansson, B.N. Reinecke, M.A. Arman, L.R. Merte, J. Kundsen, J. Schnadt, J.N. Andersen, F. Hennies, The SPECIES beamline at the MAX IV laboratory: a facility for soft X-ray RIXS and APXPS, J. Synchrotron. Radiat. 24 (2017) 344.
[27] B. Thiagarajan, Beamline Manager BLOCH, private communication (2017).
[28] A. Zakharov, Beamline Manager MAXPEEM, private communication (2017).
[29] H. Onuki, P. Elleaume, Undulators, Wigglers, and their Applications, 2003 (Chapter 3).
[30] W. Grizolli, Optical Studies for Synchrotron Radiation BeamlineS - Ray Optics, Polarization and Wave Optics (Ph.D. thesis), Lund University, 2015.
[31] K.J. Kim, Optical and power characteristics of synchrotron radiation sources, Opt. Eng. 34 (1995) 2.
[32] C. Sun, M. Hertlein, J. Kirz, M.A. Marcus, G. Portmann, D.S. Robin, C. Steier, Pseudo single bunch with adjustable frequency, in: Proceedings of North American Particle Accelerator Conference, Pasadena, 2013, p. 285, MOPHO22.
[33] OPA, Lattice design code by Andreas Streun, available for download at http://ados.web.psi.ch/opa.
[34] Tracy-3, Self-Consistent charged particle beam tracking code based on a symplectic integrator by Johan Bengtsson, available for download at https://github.com/jbengtsson/tracy-3.5.
[35] K. Wille, The Physics of Particle Accelerators - An Introduction, Oxford University Press, 2000.
[36] DIMAD, Tracking code, Manual by R. Servranckx, 2002, unpublished.
[37] Accelerator Toolbox, collection of tools to model storage rings and beam transport lines in MATLAB, available for download at http://atcollab.sourceforge.net/.
[38] E. Al Dmour, private communication 2017.
[39] B. Nash, N. Carmignani, L. Farvacque, S.M. Liuzzo, T. Perron, P. Raimondi, R. Versteegen, S. White, New Functionality for Beam Dynamics in Accelerator Toolbox (AT), in: Proceedings of International Particle Accelerator Conference, Richmond, 2015, MOPWA014.
[40] K. Klementiev, R. Chernikov, Powerful scriptable ray tracing package xrt, in: Proc. SPIE 9209, Advances in Computational Methods for X-ray Optics III, 2014, p. 92090A. http://dx.doi.org/10.1117/12.2061400.
[41] K. Kim, Characteristics of synchrotron radiation, in: AIP Conference Proceedings, Vol. 184, 1989, p. 565.
[42] S. Kwiatkowski, K. Baptiste, W. Barry, J. Julian, R. Low, D. Plate, G. Portmann, D. Robin, Camshaft bunch kicker design for the ALS storage ring, in Proceedings of European Particle Accelerator Conference, Edinburgh, 2006, p. 3547, THPLS114.
[43] S. De Santis, W. Barry, S. Kwiatkowski, T. Luo, C. Pappas, L. Reginato, D. Robin, C. Steier, C. Sun, H. Tarawneh, W.L. Waldron, Injection/extraction kicker for the ALS-U project, in: Proceedings of International Particle Accelerator Conference, Dresden, 2014, p. 3547, WEPRO016.
[44] C. Pappas, S. De Santis, J.E. Galvin, L.L. Reignato, C. Steier, C. Sun, H. Tarawneh, W.L. Waldron, Fast kicker system for ALS-U, in: Proceedings of International Particle Accelerator Conference, Dresden, 2014, p. 564, MOPME083.
[45] D. Robin, G. Portmann, F. Sannibale, W. Wan, Novel schemes for simultaneously satisfying high flux and dynamics experiments in a synchrotron light source, in: Proceedings of European Particle Accelerator Conference, Genoa, 2008, p. 2100.
[46] J.B. Murphy, S.L. Kramer, First observation of simultaneous alpha buckets in a Quasi-isochronous storage ring, Phys. Rev. Lett. 84 (2000) 24.